Synthesis of Silica-Supported Compact Phosphines and Their Application to Rhodium-Catalyzed Hydrosilylation of Hindered Ketones with Triorganosilanes

Go Hamasaka,[†] Soichiro Kawamorita,[†] Atsuko Ochida,[†] Ryuto Akiyama,[†] Kenji Hara,[‡] Atsushi Fukuoka,[‡] Kiyotaka Asakura,[‡] Wang Jae Chun,[§] Hirohisa Ohmiya,[†] and Masaya Sawamura*,[†]

Department of Chemistry, Faculty of Science, Hokkaido University, Sapporo 060−0810, Japan, Catalysis Research Center, Hokkaido University, Sapporo 001−0021, Japan, and Division of Natural Sciences, International Christian University, Mitaka, Tokyo 181−8585, Japan

Received July 18, 2008

Solid-supported phosphine ligands silica−SMAPs {[silica gel 60N]−SMAP (**1a**) or [CARiACT Q-10]−SMAP (**1b**)}, which are composed of a caged, compact trialkylphosphine (SMAP) as a ligand and silica gel (silica gel 60N or CARiACT Q-10) as a support, were synthesized through surface functionalization. The supported phosphines (**1a**,**b**) were structurally characterized by solid-state ^{13}C, ^{29}Si, and ^{31}P cross-polarization/magic angle spinning (CP/MAS) NMR spectroscopies and N_2 adsorption measurements. Complexation of **1a**,**b** with $[RhCl(cod)]_2$ afforded a mono(phosphine)-rhodium complex Silica−SMAP−RhCl(cod) exclusively, even in the presence of excess ligands, as proved by solid-state ^{13}C and ^{31}P CP/MAS NMR spectroscopies and Rh K-edged X-ray absorption fine structure (XAFS) measurements. Heterogeneous catalysts that were prepared from $[RhCl(C_2H_4)_2]_2$ and **1a**,**b** showed exceptionally high catalytic activities for the reaction of sterically hindered ketones (including di-*tert*-butyl ketone) and triorganosilanes such as Et_3SiH and (*t*-Bu)Me_2SiH. The catalyst from **1b** showed no leaching of rhodium after reaction and was reusable without decrease of the activity.

Introduction

The development of heterogenized catalysts has been studied to achieve easy separation, efficient recycling, minimization of metal traces in products, and improved handling and process control for the overall lowering of costs in catalytic processes.[1] Traditional heterogeneous catalysts are rather limited in the nature of their active site, and thus in the scope of reactions that can be accomplished. Homogeneous organometallic catalysts can catalyze a much larger variety of reaction types than traditional heterogeneous catalysts, but suffer from low or difficult reusability. In more recent years, significant developments in the area of solid-phase chemistry have resulted in significant progress being made in interdisciplinary research on selective heterogeneous catalysis. In some cases, heterogeneous catalysts are even more selective than their homogeneous counterparts.[1d] Ideally, the advantages of homogeneous and heterogeneous catalysis, such as high activity and selectivity on one hand, and separation and recycling on the other, should be combined.

In particular, silica-supported ligands, prepared by the technique of silica surface functionalization, which is the grafting of organic groups onto a silanol-containing surface using a trichloro- or trialkoxy-organosilyl groups, have been numerously reported.[2−4] A variety of ligands have been supported on silica gel and applied to various reactions; however, in many cases, the performance of catalytic activity and selectivity were only comparable with the corresponding soluble catalysts or were decreased, owing to limited accessibility of the active site of the supported catalyst, and due to the leaching of metal.

We have designed a new solid-supported ligand silica−SMAP, consisting of caged trialkylphosphine (SMAP)[5−7] and silica gel as a ligand and a support, respectively.[8] The feature of the SMAP group is that the steric environment of the phosphorus atom is extremely compact, the bicycle[2.2.2]octane framework is rigid, and the *Si*-substituents can be transformed to a wide variety of functional groups due to the reactivity of organosilicon compounds.[6] It is noted that the third feature can be utilized for the preparation of silica gel-supported phosphine. In general, silica gel-supported phosphines are prepared by silane coupling with a trialkoxysilyl group and the surface silanols of silica gel,

* To whom correspondence should be addressed. E-mail: sawamura@sci.hokudai.ac.jp.
[†] Faculty of Science, Hokkaido University.
[‡] Catalysis Research Center, Hokkaido University.
[§] International Christian University.

(1) (a) Lindner, E.; Schneller, T.; Auer, F.; Mayer, H. A. *Angew. Chem., Int. Ed.* **1999**, *38*, 2154–2174. (b) Wight, A. P.; Davis, M. E. *Chem. Rev.* **2002**, *102*, 3589–3614. (c) Valkenberg, M. H.; Hölderich, W. F. *Catal. Rev.* **2002**, *44*, 321–374. (d) Heitbaum, M.; Glorius, F.; Escher, I. *Angew. Chem., Int. Ed.* **2006**, *45*, 4732–4762.

(2) (a) Czaková, M.; Čapka, M *J. Mol. Catal.* **1981**, *11*, 313–322. (b) Michalska, Z. M.; Čapka, M.; Stoch, J. *J. Mol. Catal.* **1981**, *11*, 323–330.

(3) Liu, A. M.; Hidajat, K.; Kawi, S. *J. Mol. Cat. A* **2001**, *168*, 303–306.

(4) (a) Fetouaki, R.; Seifert, A.; Bogza, M.; Oeser, T.; Blümel, J. *Inorg. Chim. Acta* **2006**, *359*, 4865–4873. (b) Bogza, M.; Oeser, T.; Blümel, J. *J. Organomet. Chem.* **2005**, *690*, 3383–3389. (c) Merckle, C.; Blümel, J. *Top. Catal.* **2005**, *34*, 5–15.

(5) SMAP: Abbreviated to silicon-constrained monodentate trialkylphosphine: Ochida, A.; Hara, K.; Ito, H.; Sawamura, M. *Org. Lett.* **2003**, *5*, 2671–2674.

(6) For functionalization of SMAP, see: Ochida, A.; Ito, S.; Miyahara, T.; Ito, H.; Sawamura, M. *Chem. Lett.* **2006**, *35*, 294–295.

(7) Ochida, A.; Hamasaka, G.; Yamauchi, Y.; Kawamorita, S.; Oshima, N.; Hara, K.; Ohmiya, H.; Sawamura, M. *Organometallics* **2008**, *27*, 5494–5503.

(8) Hamasaka, G.; Ochida, A.; Hara, K.; Sawamura, M. *Angew. Chem., Int. Ed.* **2007**, *46*, 5381–5383.

10.1021/om800683g CCC: $40.75
Publication on Web 11/18/2008

Scheme 1. Preparation of Silica−SMAPs (1a,b)

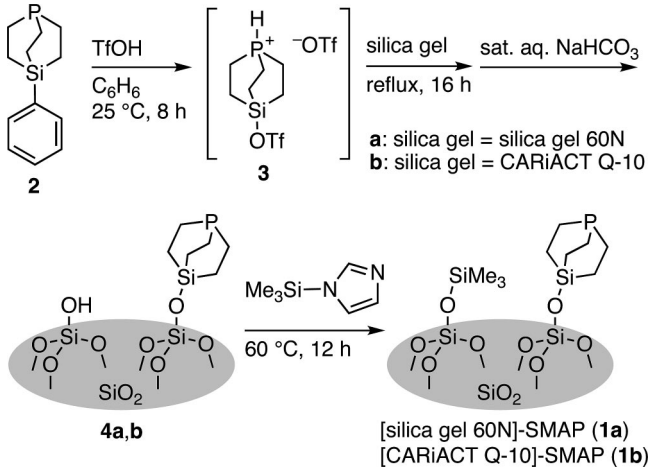

which requires the attachment of an *Si*-terminated pendant to the phosphine moiety, while silica gel-supported SMAPs (silica−SMAPs) are directly prepared by the reaction of silyl cation species, which is prepared from Ph-SMAP treated with TfOH, and silica gel surface.[8]

Because of the lack of a linker and the rigidity of the SMAP molecule, the mobility of the supported SMAP ligand will be highly restricted. Since an Si−O−Si triad (disiloxane) generally forms an angle considerably widened toward pseudo linear arrangement, the SMAP moiety will stand up on the surface, turning its phosphorus lone pair upward.[9] Metal complexation of such a supported ligand will result in the selective formation of a 1:1 metal−phosphine complex. Moreover, the phosphine ligand is extremely compact and the steric effect of the silica support will be negligible in the vicinity of the metal center. On the basis of these considerations, we envisioned that 1:1 metal−phosphine complexes prepared in this manner would serve as useful heterogeneous catalysts with extraordinary catalytic features due to the creation of sparse catalytic environment. This article reports details of our studies on the synthesis of the silica gel-supported phosphines Silica−SMAPs, their coordination properties toward 1:1 phosphine−rhodium(I) complexes, and the Rh-catalyzed hydrosilylation of ketones, in which Silica−SMAP−Rh complexes showed exceptionally high catalytic activities and broad scopes toward the reactions of sterically hindered substrates.[10]

Results and Discussion

Preparation of Silica Gel-Supported SMAPs. The heterocyclic cage of SMAP was grafted on a silica gel surface through a direct connection between the cage and a surface oxygen atom, as shown in Scheme 1. Treatment of Ph-SMAP (**2**) with TfOH in benzene afforded silyl triflate **3**,[6] which was treated with HCl-activated[11] silica gel 60N (Kanto Chemical Co., Flash chromatography grade, spherical, 40−100 μm) or CARiACT Q-10 (Fuji Silysia Co., Catalyst grade, 75−150 μm) in refluxing benzene. Filtration and elution of soluble materials and subsequent neutralization with saturated sodium hydrogen carbonate aqueous solution gave phosphine-functionalized silica gel (**4a** or **4b**). The surface silanols that remained intact were end-capped with a Me_3Si group to give [silica gel 60N]−SMAP (**1a**) or [CARiACT Q-10]−SMAP (**1b**). The amount of supported SMAP was calculated to 0.19 or 0.07 mmol/g, respectively, based on the amount of RhCl(cod) fragment that the phosphines can support through a P−Rh coordination (*vide infra*). These values correspond to surface P-densities of 0.24 and 0.19 nm^{-2}, respectively, on the basis of the surface areas determined by N_2 adsorption measurements (**1a**, 473 $m^2\ g^{-1}$; **1b**, 220 $m^2\ g^{-1}$; *vide infra*).

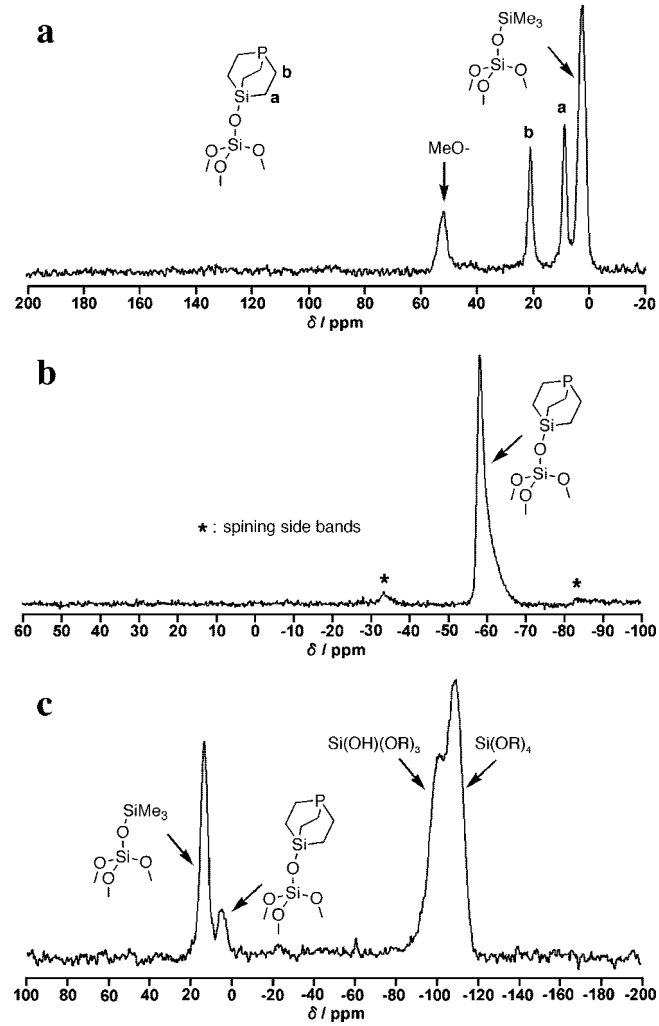

Figure 1. CP/MAS NMR spectra of [silica gel 60N]−SMAP (**1a**) for ^{13}C (a), ^{31}P (b), and ^{29}Si (c) nuclei.

Solid-State NMR Spectra of Silica Gel-Supported SMAP. The silica gel-supported SMAPs **1a** and **1b** were analyzed by solid-state ^{13}C, ^{31}P, and ^{29}Si CP/MAS NMR spectroscopies.[12] The spectra for **1a** are given in Figure 1. Spectra for **1b** are similar to those of **1a**, and are given in Supporting Information (Figures S1−S3).

The ^{13}C CP/MAS NMR spectrum of **1a** is shown in Figure 1a. A broad singlet signal (a) for the carbon atom adjacent to the silicon atom in the SMAP moiety and a signal (b) for the carbon adjacent to the phosphorus atom were observed at 7 ppm and 21 ppm, respectively. A peak was observed at 3 ppm, which corresponds to the Me_3Si groups that end-capped silanol groups. A peak at 55 ppm is deduced to absorbed MeOH or covalently bound MeO group (MeO−[SiO_2]).[13]

(9) Our search of Cambridge Structural Database for $Me_3Si-O-Si(O-)_3$ hit five molecules with appropriate structures. Angles of the 38 independent Si−O−Si triads vary from 143.13 to 172.49° with an average value of 153.84°.

(10) Part of this work has been published. See, ref 8.

(11) Rechavi, D.; Lemaire, M. *Org. Lett.* **2001**, *3*, 2493–2496.

(12) Blümel, J. *Coord. Chem. Rev.* **2008**, *252*, 2410–2423.

(13) Blümel, J. *J. Am. Chem. Soc.* **1995**, *117*, 2112–2113.

Chart 1. Model Compound for Silica−SMAP (5)

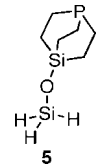

5

Table 1. Results of DFT Calculations for Various Tertiary Phosphines

entry	phosphine	V_{min}(kcal mol^{-1})	average C−P−C angle (deg)[a]
1[b]	$(t\text{-Bu})_3$P	−45.48	107.5
2[b]	$(i\text{-Pr})_3$P	−44.47	101.6
3[b]	Et_3P	−43.51	99.5
4[c]	Ph-SMAP (**2**)	−43.14	99.7
5[b]	Me_3P	−43.02	99.4
6	H_3SiO-SMAP (**5**)	−41.34	99.8
7[b]	Me_2PhP	−40.41	
8[b]	$MePh_2$P	−36.76	

[a] Values for optimized structures. [b] Data taken from ref 14. [c] Data taken from ref 5.

The ^{31}P CP/MAS NMR spectrum of **1a** shows only one broad resonance at −58 ppm (Figure 1b). This resonance can be assigned to the P atom of the SMAP moiety, by comparison with that of the ^{31}P NMR spectrum of Ph-SMAP (**2**) in C_6D_6 at −59.2 ppm. The absence of resonance for a phosphine oxide indicates that the P atom of the SMAP moiety on the silica surface has high stability against aerobic oxidation.

The ^{29}Si CP/MAS NMR spectrum of **1a** shows four peaks (Figure 1c). The peak at the highest field (−110 ppm) corresponds to the Q^4 site ($\boldsymbol{Si}(OR)_4$) on the silica gel support. The Q^3 site ((OH)$\boldsymbol{Si}(OR)_3$) (unmodified silanols) was observed at −98 ppm. The peak of the bridgehead silicon atom of the SMAP framework was observed at 4 ppm, and was assigned to $R_3\boldsymbol{Si}(OR)$. This result suggests that the SMAP is combined to silica gel by Si−O−Si covalent bonding. The peak at 13 ppm is assigned to the Me_3Si group. Prolonging the Me_3Si-end capping reaction time caused no decrease of the unmodified silanol; therefore the difficulty in the reagent accessing crowded silanol sites, such as the internal site in the silica gel, is attributed to the residual silanol functionality.

Electronic Properties. Density functional theory (DFT) calculations [B3LYP/6−31G(d,p)] were performed for the model compound H_3SiO-SMAP (**5**, Chart 1) due to the appearance of the electron-donating ability of silica gel supported SMAP (**1**). Donor ability of **5** was estimated by the value of the molecular electrostatic potential minimum V_{min} (kcal/mol) that was calculated by the optimized geometry of **5**.[14] A larger negative V_{min} value corresponds to the stronger electron-donating ability of a phosphine. As shown in Table 1, the V_{min} (−41.34 kcal/mol) of **5** is much more negative than that of monoaryldialkylphosphine Me_2PhP; however, it is less negative than that of **2**. Therefore, Silica−SMAPs (**1a**,**b**) are less electron-donative than Ph-SMAP (**2**) and Me_3P, but it should still be classified to strongly electron-donative phosphine.

Nitrogen Adsorption. Nitrogen adsorption was measured in order to estimate the bulk structure of the supports (silica gel 60N, spherical, 40−100 μm and CARiACT Q-10, catalyst grade, 75−150 μm) and the supported ligands {[silica gel 60N]−SMAP (**1a**) and [CARiACT Q-10]−SMAP (**1b**)}. Adsorption−desorption isotherms and pore diameter distributions are given in Supporting Information (Figures S4−S11). Values for the structural parameters (surface area, pore diameter and pore volume) of the supports and the ligands are summarized in Table 2. The adsorption−desorption isotherms showed hysteresis curve, thus the all samples have meso pore. In addition, these hysteresis patterns indicated typical silica gel pattern.

Table 2. Structural Parameters of Supports and Ligands

entry	material	surface area (BET, m^2 g^{-1})	pore diameter (nm)	pore volume (mL g^{-1})
1	silica gel 60N	524	5.6	0.88
2	[silica gel 60N]−SMAP (**1a**)	473	5.6	0.72
3	CARiACT Q-10	284	17.8	1.32
4	[CARiACT Q-10]−SMAP (**1b**)	220	17.3	1.08

Scheme 2. Conversion of Silica−SMAPs into Rh(I) Complexes

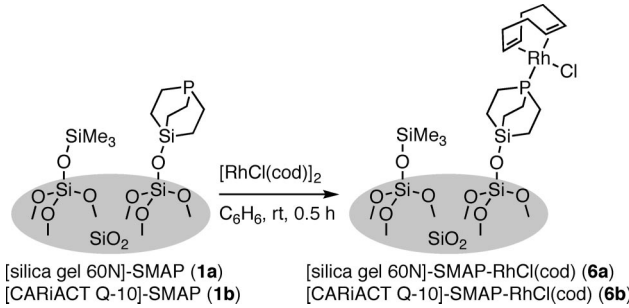

[silica gel 60N]-SMAP (**1a**)
[CARiACT Q-10]-SMAP (**1b**)

[silica gel 60N]-SMAP-RhCl(cod) (**6a**)
[CARiACT Q-10]-SMAP-RhCl(cod) (**6b**)

Pore diameter distributions of silica gel 60N and **1a** showed the relatively sharp distributions at about 5.6 nm (Table 2, entries 1 and 2). The pore distributions of CARiACT Q-10 and **1b** are broad at average 17.8 and 17.3 nm, respectively (Table 2, entries 3 and 4). The surface area and pore volume of **1a** (473 m^2g^{-1}, 0.72 mL g^{-1}) was decreased from that of silica gel 60N (Table 2, entries 1 and 2). Comparison of the structural parameters of CARiACT Q-10 and **1b** also provided similar results (surface area and pore volume of **1b** are 220 m^2 g^{-1} and 1.08 mL g^{-1}, respectively) (Table 2, entries 3 and 4).

On the basis of the surface area values, the surface P densities for **1a** and **1b** are calculated to be 0.24 and 0.19 nm^{-2}, respectively. These values may evoke much sparser nature of the P distribution on the silica surface than those expected from the density of the surface silanol group and the steric demand of the SMAP group [c.f. 4.2 nm^{-2} for the self-assembled monolayer of alkanethiolate SMAP sulfide on Au(111)].[15] This inconsistency may arise from structural inhomogeneity of the silica surface, which involves narrow sites where the cationic SMAP reagent is not accessible. Accordingly, it is likely that a substantive P-density of the functionalized surface is considerably higher than the calculated values.

Synthesis and Solid-State NMR Spectra of Silica−SMAP−Rh Complexes. The reaction of [silica gel 60N]−SMAP (**1a**) and [CARiACT Q-10]−SMAP (**1b**) with $[RhCl(cod)]_2$ gave silica-supported 1:1 rhodium-phosphine complexes, [silica gel 60N]−SMAP−RhCl(cod) (**6a**) and [CARiACT Q-10]−SMAP−RhCl(cod) (**6b**), respectively. In particular, the complexation was performed by treating $[RhCl(cod)]_2$ with excess **1** (Rh/P 1:1.5) in benzene at rt for 30 min (Scheme 2). The solid-supported Rh complexes (**6a**,**b**), which were yellow-colored (Figure 6a), were obtained by filtration followed by washing with benzene and drying. Unreacted $[RhCl(cod)]_2$ was quantitatively recovered from the filtrate and washings, and its weight was measured. The

(14) Suresh, C. H.; Koga, N. *Inorg. Chem.* **2002**, *41*, 1573–1578.

(15) Hara, K.; Akiyama, R.; Takakusagi, S.; Uosaki, K.; Yoshino, T.; Kagi, H.; Sawamura, M. *Angew. Chem., Int. Ed.* **2008**, *47*, 5627–5630.

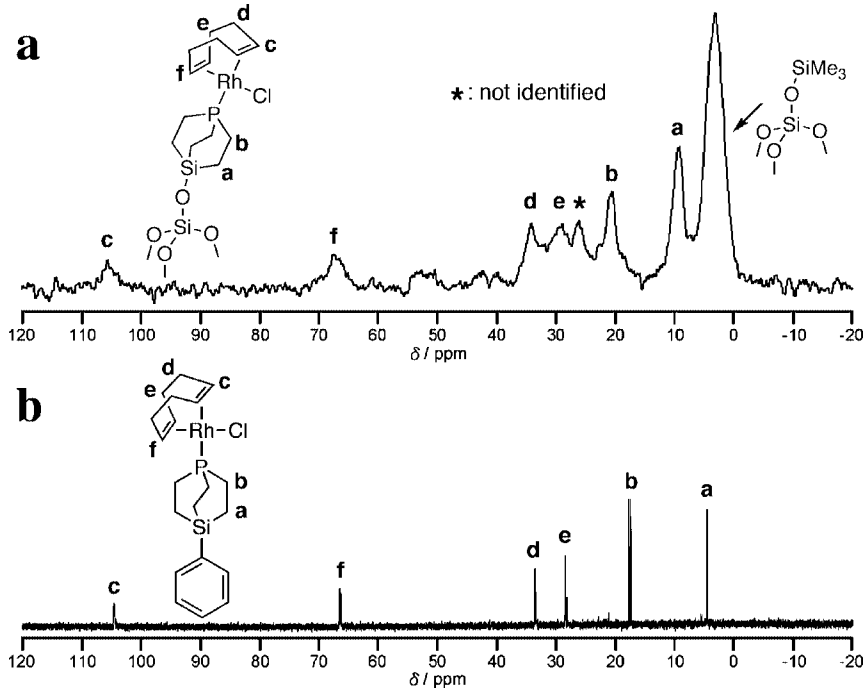

Figure 2. (a) ^{13}C CP/MAS NMR spectrum of [silica gel 60N]−SMAP−RhCl(cod) (**6a**); (b) ^{13}C NMR spectrum of [RhCl(cod)(Ph-SMAP)] (**7**) in C_6D_6.

compositions of the supported complexes (**6a**,**b**) were unambiguously determined by the solid-state NMR spectroscopies (*vide infra*). These procedures allowed determining the approximate amount of Rh loaded on the functionalized silica gel **6a** and **6b** to be 0.19 and 0.07 mmol g^{-1}, respectively, and hence the amount of P to be the same.

The solid-state ^{13}C and ^{31}P NMR spectra of **6a**,**b** were measured and compared with the solution spectra of the soluble complex [RhCl(cod)(Ph-SMAP)] (**7**), which was prepared by mixing [RhCl(cod)]$_2$ and Ph-SMAP (**2**) in C_6D_6. The ^{13}C CP/MAS NMR spectrum for **6a** is in good agreement with that of **7** (Figure 2). These spectra displayed two peaks for the sp^2 carbons on the 1,5-cyclooctadiene (cod) ligand, one of which is in the *cis* position toward the phosphine ligand, and the other is in the *trans* position. These results suggest that one 1,5-cyclooctadiene, one Cl and one phosphine ligand are bound to the Rh center, thus the formation of four-coordinated 16-electron mono(phosphine)−rhodium complex is shown.

The ^{31}P CP/MAS NMR spectrum of **6a** and the ^{31}P NMR spectrum of **7** ($^1J_{P-Rh}$ = 148 Hz) in C_6D_6 are displayed in Figure 3. These spectra show that the spectrum of **6a** is consistent with that of **7**, and indicate that **6a** has the same phosphorus environment as **7**. In addition, free phosphine was not observed; thus, all of the phosphine centers are bound to the rhodium center.

Solid-state NMR spectra of **6b** are similar to that of **6a**. These results suggested that the mono(phosphine)−rhodium complex was also formed from **1b**, and change of the support did not affect the complexation (see also Supporting Information, Figures S12, S13).

XAFS Analysis of Silica−SMAP−Rh Complex. X-ray absorption near-edge structure (XANES) spectra and imaginary parts of k^3-weighted extended X-ray absorption fine structure (EXAFS) spectra for [RhCl(cod)(**1b**)] (**6b**) are shown in Figure 4. Curve-fitting analysis of EXAFS with the double shells model (C, and P/Cl, based on the assumption that the electron density of P shell is similar enough to that of Cl shell) afforded the results summarized in Table 3. The coordination number (*N*) of Rh−C and Rh−P (or Rh−Cl) for **6b** are valued to be 3.6 and 1.6, respectively. These values are consistent with the corresponding theoretical values for [RhCl(cod)(PR$_3$)] where N(Rh−C) = 4, N(Rh−P) = 1 and N(Rh−Cl) = 1. In addition, the spectra of **6b** are similar to that of [RhCl(cod)(**2**)] (**7**) in both XANES and EXAFS regions, which indicates that **6b** has quite similar coordination environment of Rh with that of mono(phosphine)−Rh complex **7**. The similarity found in the XAFS analyses shown here is in accordance with the similarity in solid-state NMR analyses (*vide supra*).

Complexation with Excess Ligand. The effect of excess ligand toward complexation was studied by ^{31}P CP/MAS NMR spectroscopies for the sample obtained by the reaction of [RhCl(cod)]$_2$ and an excess amount of **1a** (Rh/P 1:2.1) in benzene followed by filtration and drying (Figure 5). The NMR spectrum consists of signals for both the free phosphine and the Rh-coordinated phosphine, indicating that the heterogeneous ligand **1** exclusively forms the mono(phosphine)-rhodium complex even in the presence of excess free phosphine.

Effect of the immobilization was critical for the monocoordinating property of the compact trialkylphosphine. The reaction of [RhCl(cod)]$_2$ with Ph-SMAP (**2**) in a Rh/P ratio of 1:2 gave a complex mixture, leaving no free phosphine.

Various techniques to limit the number of a phosphine ligand that coordinates to a metal center have been developed; they have generally relied on the bulkiness of the ligand.[16] In contrast, studies to develop a method to achieve selective monocoordination of a phosphine ligand with ordinary bulkiness remain partially successful.[2−4,17]

(16) (a) Christmann, U.; Vilar, R. *Angew. Chem., Int. Ed.* **2005**, *44*, 366–374. (b) Miura, M. *Angew. Chem., Int. Ed.* **2004**, *43*, 2201–2203. (c) Bellina, F.; Carpita, A.; Rossi, R. *Synthesis* **2004**, 2419–2440. (d) Tsuji, Y.; Fujiwara, T. *Chem. Lett.* **2007**, 1296–1301.

(17) For a related study, which used a bulky phosphine branched on a rigid polymer support for the Suzuki-Miyaura coupling, see: Hu, Q.-S.; Lu, Y.; Tang, Z.-Y.; Yu, H.-B. *J. Am. Chem. Soc.* **2003**, *125*, 2856–2857.

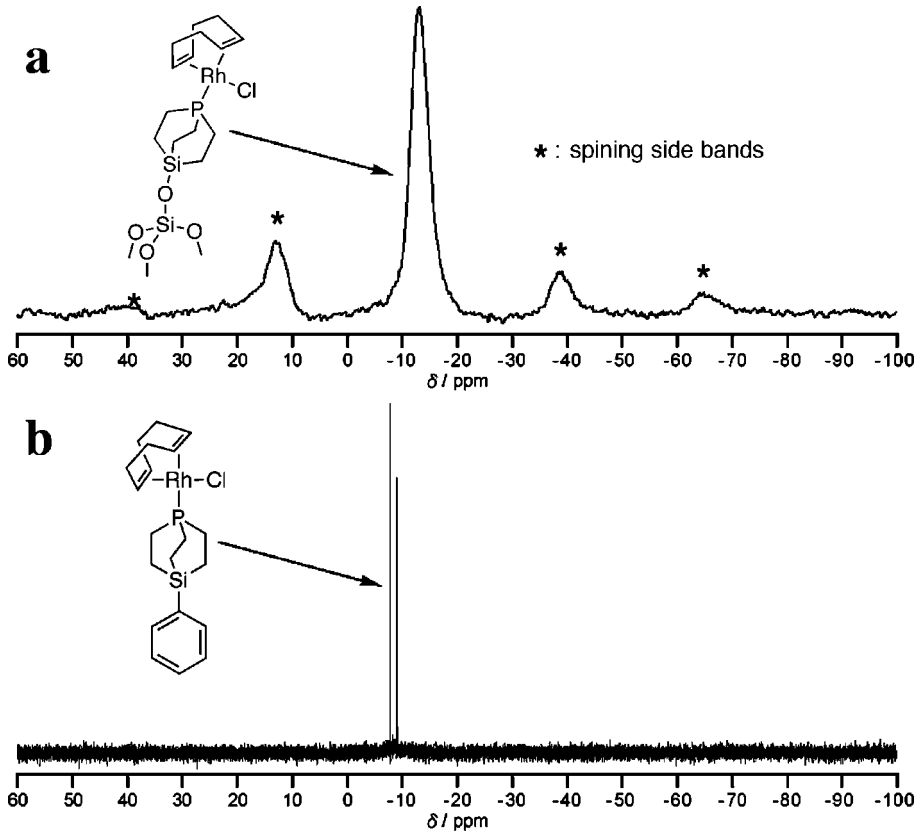

Figure 3. (a) ^{31}P CP/MAS NMR spectrum of [silica gel 60N]−SMAP−RhCl(cod) (**6a**); (b) ^{31}P NMR spectrum of [RhCl(cod)(Ph-SMAP)] (**7**) in C_6D_6.

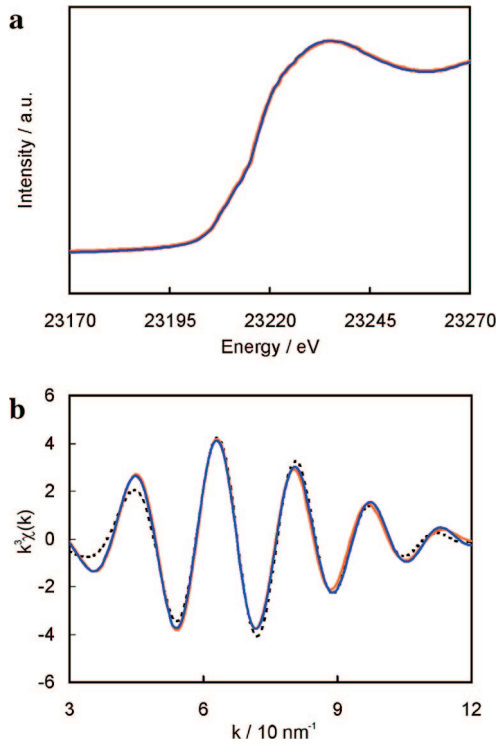

Figure 4. (a) XANES spectra of the Rh K-edge region and (b) imaginary parts of k^3-weighted Rh K-edge EXAFS oscillations for [CARiACT Q-10]−SMAP−RhCl(cod) (**6b**) (blue) and [RhCl(cod)(**2**)] (**7**) (orange). The dashed lines in (b) represent the fitted spectra for **6b** and **7**.

Hydrosilylation of Ketones with Triorganosilanes. To demonstrate ligand characteristics of Silica−SMAPs (**1**) for catalytic application, we examined the Rh-catalyzed hydrosilylation of ketones with triorganosilanes, because critical importance of a mono(phosphine)−Rh species in this catalysis had been proposed by Tsuji.[18,19] In addition to the monocoordination effect, we expected a geminating effect of the ligand compactness on catalytic performance toward the reaction of sterically demanding substrates.

Catalytic hydrosilylation of ketones is potentially a straightforward and atom-economical protocol for the preparation of silicon-protected secondary alcohols as compared with a two-step protocol involving a ketone reduction followed by alcohol silylation with a combination of a silicon electrophile and a base. For this purpose, triorgano-monohydrosilanes are to be employed as a silylating reagent; however, the triorganosilanes have a considerable steric demand. Therefore, they are generally less reactive toward carbonyl hydrosilylation than dihydro-diorganosilanes or heteroatom-substituted hydrosilanes, which are usually used in the hydrosilylation/hydrolysis protocols for the purpose of carbonyl reduction to obtain alcohols.

Table 3. Best-Fit EXAFS Data at the Rh K-Edge

complex	pair	*N*	*r*/nm	Δ*E* /eV	*σ*/nm
[CARiACT Q-10]−SMAP−RhCl(cod) (**6b**)	Rh−C	3.6	0.21	−9.4	0.0067
	Rh−P/Cl	1.6	0.24	11	0.0067
[RhCl(cod)(**2**)] (**7**)	Rh−C	3.2	0.21	−7.9	0.0067
	Rh−P/Cl	1.7	0.24	11	0.0067

(18) (a) Niyomura, O.; Tokunaga, M.; Obora, Y.; Iwasawa, T.; Tsuji, Y. *Angew. Chem., Int. Ed.* **2003**, *42*, 1287–1289. (b) Niyomura, O.; Iwasawa, T.; Sawada, N.; Tokunaga, M.; Obora, Y.; Tsuji, Y. *Organometallics* **2005**, *24*, 3468–3475.

(19) For related studies in our group, see: (a) Ochida, A.; Sawamura, M. *Chem. Asian J.* **2007**, *2*, 609–618. (b) Ito, H.; Kato, T.; Sawamura, M. *Chem. Asian J.* **2007**, *2*, 1436–1446.

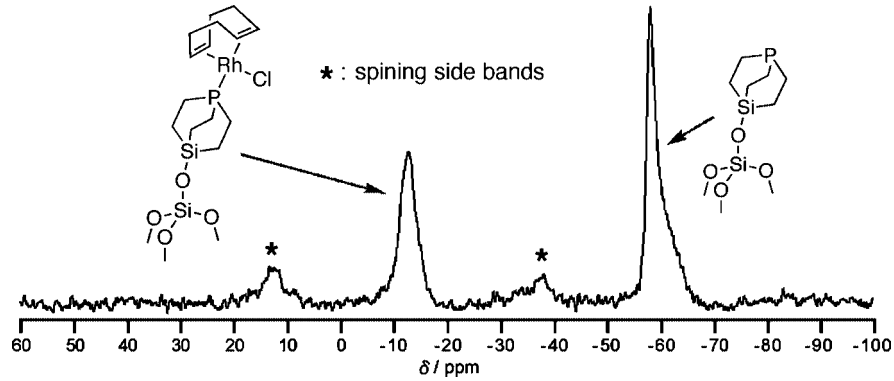

Figure 5. ^{31}P CP/MAS NMR spectrum obtained from **1a** and a substoichiometric amount of $[RhCl(cod)]_2$ (Rh/P 1:2.1).

Table 4. Hydrosilylation Catalyzed by the Rh-[Silica Gel 60N]−SMAP (1a) System

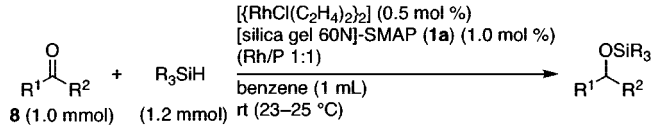

entry	ketone	silane	time[a]	yield (%)	*trans*/*cis* ratio (*endo*/*exo*)
1	**8a**	Me_2PhSiH	<5 min	93[b]	n.a.
2		Et_3SiH	<5 min	100[b]	n.a.
3		(*t*-Bu)Me_2SiH	30 min	100[b]	n.a.
4	**8b**	Me_2PhSiH	1 h	99[b]	n.a.
5		Et_3SiH	4 h	99[b]	n.a.
6		(*t*-Bu)Me_2SiH	10 h	100[b]	n.a.
7	**8c**	Me_2PhSiH	96 h	92[b]	n.a.
8		Et_3SiH	12 h	96[c]	n.a.
9		(*t*-Bu)Me_2SiH	30 h	97[c]	n.a.
10	**8d**	Me_2PhSiH	4 h	97[d]	50:50
11		Et_3SiH	2 h	98[d]	28:72
12		(*t*-Bu)Me_2SiH	12 h	99[d]	9:91
13	**8e**	Me_2PhSiH	3 h	99[d]	24:76
14		Et_3SiH	3 h	96[d]	54:46
15		(*t*-Bu)Me_2SiH	12 h	99[d]	59:41

[a] Approximate reaction time required for 100% conversion of **8**. [b] Yield based on GC analysis. [c] Isolated yield. [d] Isolated yield of diastereomer mixture.

While some copper(I)-based systems have recently been identified to be effective catalysts for the hydrosilylation with sterically demanding ketones and triorganosilanes, the catalysis required rather forcing conditions, and the substrate scope is still limited, especially for the reaction with sterically demanding silanes such as (*tert*-butyl)dimethylsilane.[15,16] Therefore, the development of efficient and general methods for the catalytic hydrosilylation of ketones with triorganosilanes is desirable.

(a) Rh-Catalyzed Hydrosilylation of Ketones with [Silica Gel 60N]−SMAP. Hydrosilylation was carried out with various combinations of ketones (**8**, 1 mmol) and triorganosilanes (1.2 mmol) in benzene at rt in the presence of silica-supported Rh catalyst (1 mol %) that is prepared *in situ* from $[RhCl(C_2H_4)_2]_2$ (0.005 mmol) and **1a** (0.01 mmol). The results are summarized in Table 4. The reactions of cyclohexanone **8a** with Me_2PhSiH and Et_3SiH were complete within 5 min (Table 4, entries 1, 2).[20] These reactions are much faster than those with the bowl-shaped phosphine (Rh/P 1:2; 3 h with Me_2PhSiH,

(20) The reaction of **1a** with $[RhCl(C_2H_4)_2]_2$ should form [silica gel 60N]−SMAP−$RhCl(C_2H_4)_2$. This catalyst precursor should release the two ethylene ligands upon rapid hydrosilylation prior to entering a catalytic cycle. Preformed, well-defined complex **6a** can also be used as equally active catalyst precursor but it needs to be aged with a hydrosilane before the addition of a ketone.

Table 5. Hydrosilylation Catalyzed by the Rh−[CARiACT Q-10]−SMAP (1b) System

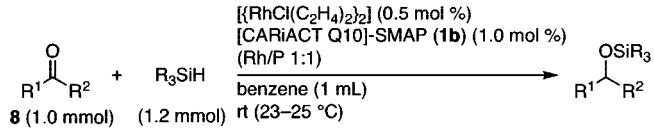

entry	ketone	silane	time[a]	yield (%)	*cis*/*trans* ratio (*endo*/*exo*)
1	 **8a**	Me_2PhSiH	<5 min	94[b]	n.a.
2		Et_3SiH	<5 min	99[b]	n.a.
3		(*t*-Bu)Me_2SiH	<5 min	99[b]	n.a.
4	 **8b**	Me_2PhSiH	10 min	100[b]	n.a.
5		Et_3SiH	1 h	99[b]	n.a.
6[c]		Et_3SiH	4 h	100[b]	n.a.
7		(*t*-Bu)Me_2SiH	4 h	100[b]	n.a.
8	 **8c**	Me_2PhSiH	42 h	94[b]	n.a.
9		Et_3SiH	4 h	96[d]	n.a.
10		(*t*-Bu)Me_2SiH	12 h	97[d]	n.a.
11	 **8d**	Me_2PhSiH	30 min	95[e]	51:49
12		Et_3SiH	1 h	91[e]	74:26
13		(*t*-Bu)Me_2SiH	2 h	100[e]	90:10
14	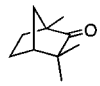 **8e**	Me_2PhSiH	30 min	100[e]	25:75
15		Et_3SiH	1 h	98[e]	54:46
16		(*t*-Bu)Me_2SiH	5 h	98[e]	58:42

[a] Approximate reaction time required for 100% conversion of **8**. [b] Yield based on GC analysis. [c] Catalyst loading, 0.1 mol % (S/C = 1000); reaction temp, 50 °C; **8b**, 5.0 mmol; Et_3SiH, 6.0 mmol; benzene, 2.5 mL. [d] Isolated yield. [e] Isolated yield of diastereomer mixture.

21 h with Et_3SiH),[18,19] which has been identified as one of the most effective ligands that promote these rhodium-catalyzed transformations. The Rh−**1a** catalyst system is also applicable to hydrosilylation with (*t*-Bu)Me_2SiH (30 min, 100% yield; Table 4, entry 3).

Replacing cyclohexanone (**8a**) with much bulkier diisopropyl ketone (**8b**) caused considerable decrease of the rate, but the reactions with Me_2PhSiH, Et_3SiH and (*t*-Bu)Me_2SiH produced the corresponding silyl ethers in quantitative yields with reasonable reaction times (1−10 h) (Table 4, entries 4−6). The catalysis with **1a** tolerates the hydrosilylations of even more challenging substrate, di-*tert*-butyl ketone (**8c**), while longer reaction times [Me_2PhSiH, 96 h; Et_3SiH, 12 h; (*t*-Bu)Me_2SiH, 30 h] were necessary for complete conversion (Table 4, entries 7−9).

Hindered, substituted cyclic ketone **8d** also underwent hydrosilylation with Me_2PhSiH, Et_3SiH and (*t*-Bu)Me_2SiH (Table 4, entries 10−12). The reaction afforded a mixture of diastereomers in different ratios depending on the silicon substituents, in which higher *cis*-selectivity was observed for bulkier silyl groups (-$SiMe_2Ph$, 50%; -$SiEt_3$, 72%; -Si(*t*-Bu)Me_2, 91%). Hydrosilylation of hindered bicyclic ketone, **8e**, with Me_2PhSiH, Et_3SiH and (*t*-Bu)Me_2SiH proceeded within reasonable reaction times (Table 4, entries 13−15). The *endo*/*exo* selectivity was dependent upon the bulkiness of the silanes; specifically, a bulky hydrosilane favored the formation of the less stable *endo*-silyl ether.

Generally, the increases of steric demand in both the ketones and the hydrosilanes (going from Me_2PhSiH to (*t*-Bu)Me_2SiH) caused the decrease of the speed of the reactions. In this context, the case of the reaction of di-*tert*-butyl ketone (**8c**) with Me_2PhSiH is exceptional.

(b) Rh-Catalyzed Hydrosilylation of Ketones with [CARiACT Q-10]−SMAP. Table 5 summarizes the results of the hydrosilylation with [CARiACT Q-10]−SMAP (**1b**) that were obtained with the same set of the substrate couples under the conditions identical to those with **1a**. The change of silica support from silica gel 60N to CARiACT Q-10 caused significant shortening of the reaction time for all substrate couples. For example, the reaction of di-*tert*-butyl ketone (**8c**) and (*t*-Bu)Me_2SiH, the most sterically demanding and challenging case, proceeded smoothly at rt with 1 mol % catalyst loading, completing in 12 h (Table 5, entry 10). Furthermore, loading of the catalyst (Rh-**1b**) could be reduced to 0.1 mol % for the reaction of diisopropyl ketone (**8b**) and Et_3SiH by the slight increase of the reaction temperature (50 °C) and the concentration (Table 5, entry 6).

Overall, it is noted that the results with [CARiACT Q-10]−SMAP (**1b**) (Table 5) is similar to those with [silica gel 60N]−SMAP (**1a**) (Table 4) both in the reactivity patterns of the substrate couples depending on their steric demands and in the diastereoselectivity patterns depending on the hydrosilanes in the reaction of the chiral ketones **8d** and **8e**. In particular,

the exceptionally low reactivity of the hydrosilylation with di-*tert*-butyl ketone (**8c**) and Me_2PhSiH is a common feature in the both catalytic systems. Accordingly, it seems that the difference of the silica supports does not influence the catalytic environment in the vicinity of the metal center but affect substrate accessibility to the catalytic center. The [CARiACT Q-10]−SMAP−Rh system, featuring larger pore size, is more efficient than the [silica gel 60N]−SMAP−Rh system with regard to the speed of conversion.

In the context of the applicability toward sterically hindered substrates, the previous studies with copper(I)-based catalytic systems are to be noted. Lipshutz and co-workers have shown that CuCl/NaOMe/diphosphine catalyst systems are effective for hydrosilylations with (*t*-Bu)Me_2SiH for specifically reactive ketones, such as methyl alkyl ketones (alkyl = primary alkyl), 2-methylcyclohexanone, and a methyl aryl ketone.[21] Typically, the reaction of benzylacetone and (*t*-Bu)Me_2SiH (1.2 eq) was performed with 0.5 mol % CuCl, 3 mol % NaOMe (Cu/base 1:6) and 0.1 mol % DM-Segphos (toluene, rt, <3 h, 99% yield). However, the applicability of this catalytic system toward more hindered ketones has not been studied. Nolan and co-workers have used Cu(I)-*N*-heterocyclic carbene complexes for the hydrosilylation of hindered ketones with Et_3SiH.[22] In particular, the hydrosilylation of di-*tert*-butyl ketone (**8c**) was performed under rather forcing conditions. The reaction of **8c** with 3 equiv of Et_3SiH in the presence of 3 mol % of (ICy)CuCl (ICy: 1,3-dicyclohexyl-2-imidazolin-2-ylidene ligand) and 12 mol % of NaO(*t*-Bu) in toluene at 80 °C achieved 96% conversion after 9 h, 96% (c.f. Table 5, entry 9; 1 mol % of Rh, rt, 4 h, 100% conv); however, its applicability using hindered silanes, such as (*t*-Bu)Me_2SiH, has yet to be demonstrated.

(c) Hydrosilylation of Heteroaromatic Ketones. As an initial study to expand the scope of our protocol toward the functionalized compounds, the hydrosilylation of simple heteroaromatic ketones (acetylated heteroaromatic compounds, **8f-i**) and the triorganosilanes with different steric demands was performed using the Rh−**1b** system (1 mol % of Rh, benzene, rt) (Table 6). The hydrosilylation of 2-acetylpyridine (**8f**) with Et_3SiH and (*t*-Bu)Me_2SiH proceeded rapidly (<5 min) to afford the corresponding silyl ethers quantitatively, while the reaction with Me_2PhSiH required longer reaction time (1 h) (Table 6, entries 1−3). The *N*-substituted pyrrole derivative **8g** was less reactive than the pyridine derivative **8f**, but the reactions with Me_2PhSiH, Et_3SiH and (*t*-Bu)Me_2SiH proceeded smoothly (2−4 h) and quantitatively (Table 6, entries 4−6). The reactions between 2-acetylfurane (**8h**) and Me_2PhSiH, Et_3SiH and (*t*-Bu)Me_2SiH proceeded rapidly (<5 min, <5 min and 15 min, respectively) (Table 6, entries 7−9). The catalyst tolerated the existence of the sulfur atom in the ketone; the reaction of 2-acetylthiophene (**8i**) with Me_2PhSiH, Et_3SiH and (*t*-Bu)Me_2SiH proceeded smoothly to complete in <5 min, 3 and 24 h, respectively (Table 6, entries 10−12).

(d) Leaching and Reusability. The bond between the P atom of **1** and the Rh atom is fairly robust, and the color of the solution phase showed no indication of metal reaching throughout the heterogeneous reaction in all cases examined in this study (Figure 6). In fact, leaching of Rh after the reaction ([silica gel 60N]−SMAP (**1a**)−Rh system; Table 4, entry 6) was below the quantification limit of the inductively coupled plasma-atomic emission spectroscopy (ICP-AES) analysis (<0.1% of the catalyst loading). The [silica gel 60N]−SMAP−Rh catalyst could be recovered by filtration (Figure 6c) and be reused for the same transformation (100% conv of **8b** with 1.2 eq of (*t*-Bu)Me_2SiH, rt, 10 h, six times, total TON = 700). Similar experiments with [CARiACT Q-10]−SMAP (**1b**)−Rh system showed the identical reusability (100% conversion of **8b** with 1.2 equiv of (*t*-Bu)Me_2SiH, rt, 4 h, five times, total TON = 600). The reaction times applied for each run (10 h with **1a**−Rh, 4 h with **1b**−Rh) were those required for 100% conversion in the first run (8 h, 96% with **1a**−Rh; 3 h 95% with **1b**−Rh). Therefore, these experiments indicated that the catalytic activity did not decrease upon the recycling.

(e) Comparison of Homogeneous and Heterogeneous Systems. It should be noted that the homogeneous system prepared from Ph-SMAP (**2**) and $[RhCl(C_2H_4)_2]_2$ (P/Rh 1:1) showed fairly high activity for the hydrosilylation of reactive ketones such as cyclohexanone (**8a**) with Me_2PhSiH (1 mol % catalyst; 30 min, 85% conv; 1 h, 100% conv) as compared to

Table 6. Hydrosilylation of Heteroaromatic Ketones Catalyzed by the Rh−[CARiACT Q-10]−SMAP (1b) System

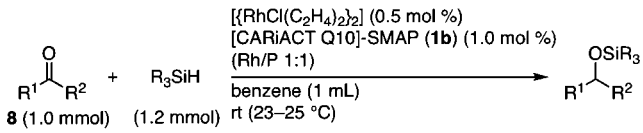

entry	ketone	silane	time[a]	yield (%)[b]
1	 **8f**	Me_2PhSiH	1 h	96
2		Et_3SiH	<5 min	98
3		(*t*-Bu)Me_2SiH	<5 min	97
4	 **8g**	Me_2PhSiH	4 h	100
5		Et_3SiH	2 h	97
6		(*t*-Bu)Me_2SiH	2 h	98
7	 **8h**	Me_2PhSiH	<5 min	100
8		Et_3SiH	<5 min	99
9		(*t*-Bu)Me_2SiH	15 min	98
10	 **8i**	Me_2PhSiH	<5 min	100
11		Et_3SiH	3 h	98
12		(*t*-Bu)Me_2SiH	24 h	96

[a] Approximate reaction time required for 100% conversion of **8**. [b] Isolated yield.

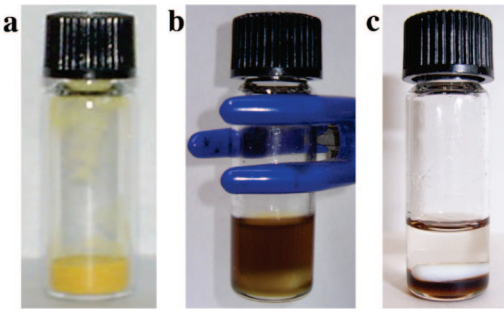

Figure 6. Photograph of stored sample of **6a** (a) and the reactor system at a time during (b) and after the reaction (c) (Table 4, entry 6).

(21) Lipshutz, B. H.; Caires, C. C.; Kuipers, P.; Chrisman, W. *Org. Lett.* **2003**, *5*, 3085–3088.

(22) (a) Díez-González, S.; Kaur, H.; Zinn, F. K.; Stevens, E. D.; Nolan, S. P. *J. Org. Chem.* **2005**, *70*, 4784–4796. (b) Díez-González, S.; Scott, N. M.; Nolan, S. P. *Organometallics* **2006**, *25*, 2355–2358.

Table 7. Hydrosilylation of 8b with (*t*-Bu)Me_2SiH with Homogeneous Catalysts

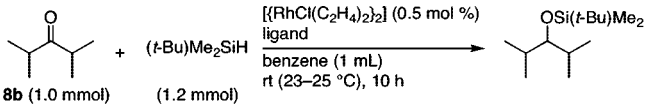

entry	ligand (mol %)	GC yield (%)
1	Ph-SMAP (**2**) (1)	0
2	Ph-SMAP (**2**) (2)	0
3	Ph_3P (1)	0
4	Ph_3P (2)	trace
5	dppe (0.5)	0
6	dppe (1)	0
7	(t-Bu)$_3$P (1)	trace
8	(t-Bu)$_3$P (2)	2

the corresponding PPh_3−Rh system (1 mol % catalyst; 3 h, 27%; 5 h, 37%).[7] The Ph-SMAP−Rh system, however, was completely inactive toward the hydrosilylation of diisopropyl ketone (**8b**) with (*t*-Bu)Me_2SiH, irrespective of the Rh/P ratio ranging from 1:1 to 1:2 (Table 7, entries 1 and 2). In addition, the catalysts (1 mol % Rh) prepared from other conventional phosphines including PPh_3, P(*t*-Bu)$_3$, and 1,2-bis(diphenylphosphino)ethane (dppe) also showed almost no activity (Table 7, entries 3−8). The most likely reason for the lower reactivity of the homogeneous catalyst systems would be the lack of a mono(phosphine)-rhodium species.

In fact, the strong tendency of compact phosphine **2** to congregate on the rhodium center was confirmed in the ^{31}P NMR spectra of a mixture of $[RhCl(C_2H_4)_2]_2$ and Ph-SMAP (**2**) (Rh/P 1:1, 1:2, 1:3, 1:4) in C_6D_6 under 1 atm of ethylene atmosphere (Supporting Information, Figures S14−S17). In the case of Rh/P 1:1 (Supporting Information, Figure S14), the signal assignment was incomplete, but the spectrum involving P−P couplings with relatively small coupling constants (δ −22.4, 3.0, 20.5; 27−31 Hz) indicates that there are considerable amounts of species that have at least two molecules of **2** on a Rh center with *cis* relationship. On the basis of the rationale that a P nucleus *trans* to a Cl ligand has a larger J_{P-Rh} value than that *trans* to P or an alkene ligand (trans influence), *trans*-[$RhCl(C_2H_4)$(**2**)$_2$] is one of the likely candidates for the species giving the major doublet signal at δ −10.5 (J_{P-Rh} = 120 Hz). In the case of Rh/P 1:2 (Supporting Information, Figure S15), the signals at δ 2.9 and 6.5 are ascribed to a Wilkinson-type complex, [$RhCl$(**2**)$_3$]. ^{31}P NMR spectra of Rh/P 1:3 and 1:4 (Supporting Information, Figures S16 and S17) show the signal for the Wilkinson-type complex (δ 2.9 and 6.5) and a broad singlet signal (Rh/P 1:3, δ −50; Rh/P 1:4, δ −54, −52). These results suggest that it is difficult to generate the mono(phosphine)−rhodium complex by mixing $[RhCl(C_2H_4)_2]_2$ and **2**.

(f) Proposed Mechanism. In general, the mechanism for hydrosilylation of ketone is explained using the Chalk-Harrod type and modified Chalk-Harrod type mechanisms.[23,24] In these mechanisms, the ketone is required to coordinate to the Rh(III) center for the reaction to proceed; however, it seems that the coordination of a sterically hindered ketone such as di-*tert*-butyl ketone (**8c**) to the Rh(III) center is difficult. Accordingly, the Chalk-Harrod type and modified Chalk-Harrod type mechanisms are not appropriate as a mechanism of the catalysis with silica−SMAP−Rh system.

Scheme 3. Proposed Mechanism for the Hydrosilylation of Sterically Hindered Ketones with Triorganosilane Catalyzed by a Silica−SMAP−Rh System

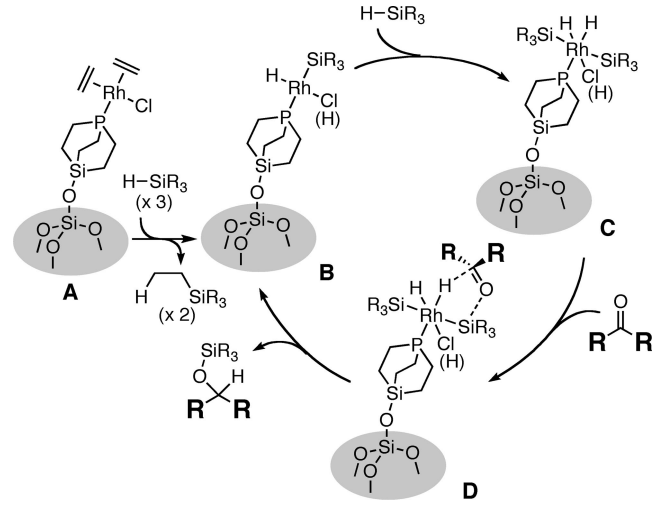

Several groups have proposed other catalytic mechanisms for hydrosilylation,[25] where the higher oxidation states, such as Rh(V),[26−28] contribute to the catalytic cycle. Accordingly, a hypothetical mechanism as illustrated in Scheme 3 might be proposed for the silica−SMAP−Rh-catalyzed hydrosilylation. The reaction of silica−SMAP (**1**) with $[RhCl(C_2H_4)_2]_2$ should form [silica]−SMAP−$RhCl(C_2H_4)_2$ (**A**). This catalyst precursor should release the two ethylene ligands upon rapid hydrosilylation and undergoes oxidative addition of a hydrosilane prior to entering a catalytic cycle as **B**. The Rh(III) species **B** undergoes further oxidative addition of a second hydrosilane to provide Rh(V) species **C**, which has two trialkylsilyl ligands. When the trialkylsilyl groups are bulky, the steric repulsion may be avoided by trans arrangement of the two groups as in **C**. The compactness and strong electron donor character of SMAP should make this step more favorable. Then, the dihydridodisilylrhodium(V) species (**C**), which is expected to be more reactive than Rh(III) species **B**, transfers a silyl group and a hydride to the ketone through the five-membered ring transition state as illustrated by **D** to give the silyl ether along with Rh(III) species **B**.

In this proposed mechanism, silyl ether is obtained without the close approach of the ketone to the Rh center; therefore, this catalytic cycle is able to explain the high catalytic activity of Silica SMAP−Rh for the hydrosilylation of sterically hindered ketones and silanes. Unfortunately, experimental data to support this mechanism has not yet been obtained.

Conclusions

Silica gel-supported SMAPs, [silica]−SMAP (**1a**) and [CARiACT Q-10]−SMAP (**1b**), consisting of a compact, bridged bicyclic trialkylphosphine were synthesized. These materials

(23) Ojima, I.; Kogure, T. *Organometallics* **1982**, *1*, 1390–1399.

(24) For theoretically investigation of Chalk-Harrod mechanism (hydrosilylation of ethylene), see: Sakaki, S.; Sumimoto, M.; Fukuhara, M.; Sugimoto, M.; Fujimoto, H.; Matsuzaki, S. *Organometallics* **2002**, *21*, 3788–3802.

(25) Ojima, I.; Li, Z.; Zhu, J. In *Recent Advances in the Hydrosilylation Reaction: Chemistry of Organosillicon Compounds*; Rappoport, Z., Apetorg, Y., Eds.; Wiley: New York, 1998; Vol. 2, pp 1687−1792.

(26) (a) Ruiz, J.; Bentz, P. O.; Mann, B. E.; Spencer, C. M.; Taylor, B. F.; Maitlis, P. M. *J. Chem. Soc., Dalton Trans.* **1987**, 2709–2713. (b) Millan, A.; Fernandez, M. J.; Bentz, P.; Maitlis, P. M. *J. Mol. Catal.* **1984**, *26*, 89–104.

(27) (a) Duckett, S. B.; Perutz, R. N. *Organometallics* **1992**, *11*, 90–98. (b) Duckett, S. B.; Haddleton, D. M.; Jackson, S. A.; Perutz, R. N.; Poliakoff, M.; Upmacis, R. K. *Organometallics* **1988**, *7*, 1526–1532.

(28) Nagashima, H.; Tatebe, K.; Ishibashi, T.; Nakaoka, A.; Sakakibara, J.; Itoh, K. *Organometallics* **1995**, *14*, 2868–2879.

were analyzed by ^{13}C, ^{29}Si, ^{31}P MAS/NMR and nitrogen adsorption measurements. The NMR spectra indicated that in **1a** and **1b** the SMAP framework is maintained and combination to the support occurs by Si−O−Si covalent bonding. Nitrogen adsorption showed that the values of specific surface area and pore diameter were significantly different between **1a** and **1b**, and were dependent on the kind of support. Mixing of **1a** or **1b** with $[RhCl(cod)]_2$ afforded [silica]−[RhCl(cod)(SMAP)] (**6a**) or [CARiACT Q-10]−[RhCl(cod)(SMAP)] (**6b**), respectively. These structures were confirmed by ^{13}C, ^{31}P CP/MAS NMR spectra and XAFS. These data demonstrate the formation of mono(phosphine)−rhodium(I) complexes. In addition, mono-(phosphine)−rhodium(I) complex was formed even in the presence of excess ligand.

[Silica]−SMAP (**1a**) and [CARiACT Q-10]−SMAP (**1b**) were applied to the rhodium-catalyzed hydrosilylation of ketones with triorganosilanes. These ligands showed an unprecedented high tolerance toward sterically hindered ketones and silanes. It appears that the high catalytic activity is caused by the selective generation of mono(phosphine)-rhodium complex, even in the presence of excess ligand. Leaching of Rh into the solution phase was below the quantification limit of ICP-AES analysis. The bond between P on SMAP and Rh is fairly strong; thus, the catalyst was recyclable without any decrease in catalytic activity. It is proposed that the monocoordinating, compact and strongly electron-donating feature of silica−SMAPs may induce the Rh(III)−Rh(V) hydrosilylation catalytic cycle.

Experimental Section

General. All manipulations involving air- and moisture-sensitive compounds were carried out under argon or nitrogen. Unless otherwise noted, materials were obtained from commercial suppliers and purified by the standard procedures. Dry THF and toluene were purchased from Kanto Chem. Co., Inc. DME was purchased from Junsei Chem. Co., Inc. and was dried with MS 4A. Dry benzene was purchased from Sigma-Aldrich, Inc. Benzene and THF were distilled from Na/benzophenone and were degassed via three freeze−pump−thaw cycles before use. Ketones and hydrosilanes were distilled from CaH_2 before use. $[RhCl(cod)]_2$[29] and $[RhCl(C_2H_4)_2]_2$[30] were prepared according to the reported procedures. Silica gel 60N (Flash chromatography grade, spherical, 40−100 μm) was purchased from Kanto Chem. Co., Inc. Activation of silica gel 60N was performed according to the reported procedure.[11] CARiACT Q-10 (Catalyst grade, 75−150 μm) was purchased from Fuji Silysia Chemical Ltd. and used as received.

Solution NMR spectra were recorded on a Varian Gemini 2000 (^1H: 300 MHz; ^{13}C: 75.4 MHz; ^{31}P: 121.4 MHz) spectrometer. Tetramethylsilane or C_6H_6 (^1H), $CDCl_3$ or C_6D_6 (^{13}C), and 85% phosphoric acid (^{31}P) were employed as internal and external standards, respectively. CP/MAS NMR spectra were recorded on a Bruker MSL-400 (^{13}C: 100.8 MHz; ^{31}P: 161.9 MHz; ^{29}Si: 79.4 MHz) spectrometer with a sample spinning rate of 4000 Hz and a decoupling power of 12 dB. Other parameters for ^{13}C, ^{31}P and ^{29}Si CP/MAS measurements were as follows, respectively: Contact time; 1 ms, 1 ms, 3 ms. $\pi/2$ pulse; 4.3 μs, 3.7 μs, 4.3 μs. Relaxation delay; 5 s, 10 s, 6 s. Elemental analyses were performed at the Center for Instrumental Analysis, Hokkaido University. High-resolution mass spectra were recorded on a JEOL JMS-GCmate mass spectrometer or JEOL JMS-700TZ mass spectrometer at the Center for Instrumental Analysis, Hokkaido University. N_2 adsorption was carried out with a Quantachrome Autosorb-6. ICP-AES analyses were performed on a Seiko Co. Ltd. model SPS 7000 in Hokkaido University.

Theoretical Calculations. All theoretical calculations were carried out using the Gaussian 03 program with density functional theory at B3LYP method. The geometry of H_3SiO-SMAP (**5**) was optimized by using 6−31G(d,p) basis set. It was confirmed that the optimized structure of **5** has a minimum energy by frequency calculations. The V_{min} calculation of **5** was performed at 6−31G(d,p).

[silica gel 60N]−SMAP (1a). Ph-SMAP (**2**) (0.82 mmol, 180 mg) was dissolved in anhydrous and degassed benzene (10 mL) under argon atmosphere. TfOH (6.5 mmol, 0.58 mL) was added at 4 °C. The solution was stirred at room temperature for 8 h and was added to an activated silica gel[11] (1.500 g) at room temperature. The suspension was refluxed for 16 h under gentle stirring, and then was filtered with a glass pipet equipped with a cotton filter. The filtered solid was washed successively with degassed benzene, degassed MeOH and degassed water. The colorless gel was then treated with degassed saturated aq. $NaHCO_3$ and was washed successively with degassed water and MeOH. Drying in vacuum first at room temperature for 3 h and then at 120 °C overnight gave **4a**. The obtained gel was treated with *N*-trimethylsilylimidazole (3.5 mL, excess) at 60 °C for 12 h, then was filtered with a glass pipet equipped with a cotton filter and washed with degassed MeOH. Drying in vacuum first at room temperature for 3 h and then at 120 °C overnight gave 1.478 g of [silica gel 60N]−SMAP (**1**, 0.20 mmol SMAP g^{-1}, 36% yield from **2**) (*vide infra* for calculation): ^{13}C CP/MAS NMR (100.8 MHz) δ 3 (br s, -OSi(CH_3)$_3$), 7 (br s, Si*C*CP), 21 (br s, SiC*C*P), 52 (br s, CH_3OH); ^{29}Si CP/MAS NMR (79.4 MHz) δ −110 (br s, Si(OR)$_4$), −98 (br s, (OH)Si(OR)$_3$), 4 (br s, SMAP), 13 (br s, -OSiMe_3); ^{31}P CP/MAS NMR (160.2 MHz) δ −58 (br s); Anal. Found: C, 7.44; H, 1.92.

[CARiACT Q-10]−SMAP (1b). This material (0.07 mmol SMAP g^{-1}, 33% yield from Ph-SMAP) was obtained by a procedure similar to that for the preparation of **1a** (*vide infra* for calculation): ^{13}C CP/MAS NMR (100.8 MHz) δ 3 (br s, -OSi(CH_3)$_3$), 9 (br s, Si *C*CP), 21 (br s, SiC*C*P), 51 (br s, CH_3OH); ^{29}Si CP/MAS NMR (79.4 MHz) δ −110 (br s, Si(OR)$_4$), −101 (br s, (OH)Si(OR)$_3$), −89 (br s, (OH)$_2$Si(OR)$_2$), 4 (br s, SMAP), 13 (br s, -OSiMe_3); ^{31}P CP/MAS NMR (160.2 MHz) δ −58 (br s); Anal. Found: C, 4.45; H, 1.18.

[Silica Gel 60N]−SMAP−RhCl(cod) (6a). In a glovebox, [silica gel 60N]−SMAP (**1a**) (480 mg, 0.096 mmol) and $[RhCl(cod)]_2$ (35.8 mg, 0.073 mmol) were placed in a vial tube. Anhydrous, degassed benzene (1 mL) was added and stirred at room temperature for 30 min. The suspension was filtered with a glass pipet equipped with a cotton filter, and the filtered solid was washed with degassed benzene: the filtrate and washings were quantitatively recovered and combined. The powder was collected in a vial tube, which was then sealed with a screw cap. The vial tube and the combined filtrate and washings were removed from the glovebox. The solution was evaporated and dried in vacuum to recover 12.0 mg (0.024 mmol) of $[RhCl(cod)]_2$. The powder was dried in vacuum at room temperature for 12 h to give 477.7 mg of **6a**, which should contain 23.8 mg (35.8−12.0 mg) of RhCl(cod). Thus, lording of the phosphine was determined to be 0.19 mmol SMAP g^{-1} based on the Rh to P stoichiometry of 1:1. This value allowed determining the loading of SMAP on [silica]−SMAP to be 0.20 mmol SMAP g^{-1} (*vide info*): ^{13}C NMR (100.8 MHz) δ 3 (br s, -OSi*C*H_3), 9 (br s, -Si(*C*H_2CH$_2$)$_3$P-), 20 (br s, -Si(CH$_2$*C*H$_2$)$_3$P-), 28 (br s, *C*H_2), 34 (br s, *C*H_2), 51 (br s, *C*H_3OH), 67 (br s, *C*H), 105 (br s, *C*H); ^{31}P NMR (160.2 MHz) δ −13 (br s).

[CARiACT Q-10]−SMAP−RhCl(cod) (6b). This material was obtained by a procedure similar to that for the preparation of **6a**: ^{13}C NMR (100.8 MHz) δ 3 (br s, -OSi*C*H_3), 9 (br s, -Si(*C*H_2CH$_2$)$_3$P-), 20 (br s, -Si(CH$_2$*C*H$_2$)$_3$P-), 28 (br s, *C*H_2), 33 (br s, *C*H_2), 51 (br s, *C*H_3OH), 66 (br s, *C*H), 104 (br s, *C*H); ^{31}P NMR (160.2 MHz) δ −12 (br s).

Preparation of [RhCl(cod)(Ph-SMAP)] (Soluble Complex, 7). Under argon atmosphere, Ph-SMAP and $[RhCl(cod)]_2$ were placed in an NMR tube. Anhydrous, degassed C_6D_6 was added and the tube

(29) Giordano, G.; Crabtree, R. H. *Inorg. Synth.* **1979**, *19*, 218–220.
(30) Cramer, R. *Inorg. Synth.* **1990**, *28*, 86–88.

was shaken. The NMR tube was sealed and was subjected to ^{1}H, ^{13}C and ^{31}P NMR measurements. [RhCl(cod)(Ph-SMAP)] (**7**) was obtained as a major product, contaminated with small amounts of unidentified materials: ^{1}H NMR (300 MHz, C_6D_6) δ 0.68−0.77 (m, 6H, -Si(CH_2CH$_2$)$_3$P-), 1.69−1.91 (m, 4H, CH$_2$), 2.07−2.14 (m, 6H, -Si(CH$_2$CH_2)$_3$P-), 2.01−2.23 (m, 4H, CH_2), 3.28−3.29 (m, 2H, C*H*), 5.71−5.72 (m, 2H, C*H*), 7.10−7.20 (m, 5H, Ar*H*); ^{13}C NMR (75.4 MHz, C_6D_6) δ 4.50 (d, J_{C-Si} = 6.9 Hz, -Si(*C*H$_2$CH$_2$)$_3$P-), 17.54 (d, J_{C-P} = 23.5 Hz, -Si(CH$_2$*C*H$_2$)$_3$P-), 28.44 (*C*H$_2$), 33.49 (*C*H$_2$), 66.46 (d, J_{C-Rh} = 14.3 Hz, *C*H), 104.38−104.64 (m, *C*H), 128.21 (*C*H), 130.11 (*C*H), 134.07 (*C*H), 134.50 (d, J_{C-Si} = 3.4 Hz, *C*); ^{31}P NMR (121.4 MHz, C_6D_6) δ −8.40 (d, J_{P-Rh} = 148 Hz).

XAFS Analysis of Rh Complexes 6b and 7. Rh K-edge XAFS spectra were measured at room temperature in NW10A station, Photon Factory Advanced Ring (PF-AR), High Energy Accelerator Research Organization (KEK) with a Si (311) double-crystal monochromator in a transmission mode. XAFS spectra were analyzed by a REX2000 program (Rigaku) and the obtained k^3-weighted EXAFS oscillations (k, 30−120 nm^{-1}) were Fourier-transformed into *R*-space and the curve-fitting analysis was performed in *R*-space (*R,* 0.11−0.25 nm). Phase shifts and backscattering amplitudes were calculated by the FEFF8 code.

General Procedure for the Hydrosilylation of Ketones Catalyzed by Rhodium(I)−Silica−SMAP. In a glovebox, silica−SMAP (**1a** or **1b**) (0.01 mmol) and [RhCl(C$_2$H$_4$)$_2$]$_2$ (0.005 mmol), internal standard (dibenzyl, 0.25 mmol) were placed in a vial tube. Anhydrous, degassed benzene (1 mL) was added, and the mixture was stirred at room temperature for a few minutes. Then, silane (1.2 mmol) and ketone (1.0 mmol) were added. After being sealed with a screw cap having a rubber septum, the vial tube was removed from the glovebox. Conversion of the reaction was checked by GLC. After the reaction completed, the mixture was applied to a short-pass silica gel column and was eluted with Et$_2$O. Yields of the products were determined by GC analysis.

Hydrosilylation of Dipropylketone (8b) Catalyzed by Rhodium(I)−Ph-SMAP (Homogeneous Catalyst). In a glovebox, ligand (0.01 or 0.02 mmol) and [RhCl(C$_2$H$_4$)$_2$]$_2$ (0.005 mmol), and an internal standard (dibenzyl, 0.25 mmol) were placed in a vial tube. Anhydrous, degassed benzene (1 mL) was added, and the mixture was stirred at room temperature for a few minutes. Then, Me$_2$PhSiH (1.2 mmol) and cyclohexanone (**8b**) (1.0 mmol) were added. After being sealed with a screw cap, the vial tube having a rubber septum was removed from the glovebox. Conversion of the reaction was checked by GLC. After the reaction completed, the mixture was applied to a short-pass silica gel column and was eluted with Et$_2$O. Yields of the products were determined by GC analysis.

ICP Measurements for Rh Leaching. After the reaction of diisopropyl ketone (**8b**) (1.0 mmol) and (*t*-Bu)Me$_2$SiH (1.2 mmol) (1 mol % Rh, Table 4, entry 6) was completed, the supernatant liquid was collected by a syringe, passed through a membrane filter (pore size 0.45 μm), and evaporated. The residue was dissolved in 60% HNO$_3$ aq. (3 mL). The solution was dried by heating, and the residue was dissolved in 0.5% HNO$_3$ aq. (10 mL). The resulting solution was subjected to ICP-AES analysis.

Recovery and Reuse of [Silica]−SMAP−Rh Catalyst. All the operations were carried out in a glovebox. After the reaction of diisopropyl ketone (**8b**) (1.0 mmol) and (*t*-Bu)Me$_2$SiH (1.2 mmol) (1 mol % Rh, Table 4, entry 6) completed, the suspension was filtered through a glass pipet equipped with a cotton filter, and was washed with anhydrous, degassed benzene. Brown-colored gel was dried on the filter through a stream of nitrogen. An internal standard (dibenzyl, 0.25 mmol) and the recovered catalyst gel were placed in the vial tube that was used for the second run. Anhydrous, degassed benzene (1 mL) was added, and the mixture was stirred at room temperature for a few minutes. Then, (*t*-Bu)Me$_2$SiH (1.2 mmol) and diisopropyl ketone (**8b**) (1.0 mmol) were added. The suspension was stirred at room temperature for 10 h, and yields of the products were determined by GC analysis to be 100%. This recycling procedure was repeated further without any decrease of the yield until total catalyst turnover number has reached to 700.

Reaction of [RhCl(C$_2$H$_4$)$_2$]$_2$ with Ph-SMAP (2) in C$_6$D$_6$. Under ethylene atmosphere, Ph-SMAP (**2**) (2.2 mg, 0.01 mmol) and [RhCl(C$_2$H$_4$)$_2$]$_2$ (1.9 mg, 0.005 mmol) were placed in an NMR tube (P/Rh = 1). Anhydrous, degassed C_6D_6 (ca. 0.8 mL) was added. The NMR tube was shaken, and was subjected to ^{31}P NMR measurement (256 scans, 15 min). After the NMR measurement, 1.9 mg of **2** (0.01 mmol) was added to the NMR tube (P/Rh = 2). The tube was shaken, and was subjected to the second run of the NMR measurement. The portion wise addition of **2** was repeated two more times for the NMR measurements at P/Rh = 3 and 4. P/Rh = 1 (Supporting Information, Figure S14): ^{31}P NMR (121.4 MHz, C_6D_6) δ −22.4 (dd, J_{P-Rh} = 117 Hz, J_{P-P} = 27 and 28 Hz), −10.5 (d, J_{P-Rh} = 120 Hz), 3.0 (dd, J_{P-Rh} = 97 Hz, J_{P-P} = 29 and 31 Hz), 20.5 (dd, J_{P-Rh} = 137 Hz, J_{P-P} = 27 Hz). P/Rh = 2 (Supporting Information, Figure S15): ^{31}P NMR (121.4 MHz, C_6D_6) δ −10.7 (d, J_{P-Rh} = 120 Hz), 2.9 (2P, dd, J_{P-Rh} = 96 Hz, J_{P-P} = 31 Hz), 6.5 (1P, ddd, J_{P-Rh} = 153 Hz, J_{P-P} = 29 and 32 Hz). P/Rh = 3 (Supporting Information, Figure S16): ^{31}P NMR (121.4 MHz, C_6D_6) δ −50 (br s), 2.9 (2P, dd, J_{P-Rh} = 97 Hz, J_{P-P} = 31 Hz), 6.5 (1P, ddd, J_{P-Rh} = 153 Hz, J_{P-P} = 29 and 32 Hz). P/Rh = 4 (Supporting Information, Figure S17): ^{31}P NMR (121.4 MHz, C_6D_6) δ −54 (br s), −52 (br s), 2.9 (dd, J_{P-Rh} = 97 Hz, J_{P-P} = 31 Hz), 6.5 (dd, J_{P-Rh} = 152 Hz, J_{P-P} = 29, 32 Hz).

2,4-Dimethyl-3-(dimethylphenylsiloxy)pentane (Table 4, entry 4). ^{1}H NMR (300 MHz, $CDCl_3$) δ 0.38 (s, 6H, -Si(CH_3)$_2$Ph), 0.80 (d, J = 6.9 Hz, 6H, -CH(CH_3)$_2$), 0.85 (d, J = 6.6 Hz, 6H, -CH(CH_3)$_2$), 1.74 (dsept, J = 5.7, 6.6, 6.9 Hz, 2H, -C*H*(CH$_3$)$_2$), 3.13 (t, J = 5.4, 1H, -C*H*OSi-), 7.35−7.37 (m, 3H, Ar*H*), 7.58−7.61 (m, 2H, Ar*H*). ^{13}C NMR (75.4 MHz, $CDCl_3$) δ −0.50 (-OSi(*C*H$_3$)$_2$Ph), 17.72 (-CH(*C*H$_3$)$_2$), 20.30 (-CH(CH$_3$)$_2$), 30.98 (-*C*H(CH$_3$)$_2$), 83.77 (-*C*HOSi-), 127.68 (*C*H), 129.24 (*C*H), 133.76 (*C*H), 139.17 (*C*). HRMS (*m*/*z*): [M]$^+$ calcd for $C_{15}H_{26}OSi$, 250.1753; found, 250.1754. Anal. calcd for $C_{15}H_{26}OSi$: C 71.93%, H 10.46%. Found: C 71.83%, H 10.54%.

2,2,4,4-Tetramethyl-3-(dimethylphenylsiloxy)pentane (Table 4, entry 7). ^{1}H NMR (300 MHz, $CDCl_3$) δ 0.39 (s, 6H, -Si(CH_3)$_2$Ph), 0.94 (s, 18H, -C(CH_3)$_3$), 3.12 (s, 1H, -C*H*OSi-), 7.34−7.36 (m, 3H, Ar*H*), 7.58−7.61 (m, 2H, Ar*H*). ^{13}C NMR (100.4 MHz, $CDCl_3$) δ −0.43 (-Si(*C*H$_3$)$_2$Ph), 29.20 (C(*C*H$_3$)$_3$), 37.70 (*C*(CH$_3$)$_3$), 88.47 (-*C*HOSi-), 127.64 (*C*H), 129.06 (*C*H), 133.67 (*C*H), 139.74 (*C*). HRMS (*m*/*z*): [M-Me]$^+$ calcd for $C_{16}H_{27}OSi$, 263.1831; found, 263.1827. Anal. calcd for $C_{17}H_{30}OSi$: C 73.31%, H 10.86%. Found: C 73.22%, H 10.75%.

3-(*tert*-Butyldimethylsiloxy)-2,2,4,4-tetramethylpentane (Table 4, entry 9). ^{1}H NMR (300 MHz, $CDCl_3$) δ 0.08 (s, 6H, -Si(CH_3)$_2$(C(CH$_3$)$_3$)), 0.94 (s, 9H, -Si(CH$_3$)$_2$(C(CH_3)$_3$)), 0.98 (s, 18H, -C(CH_3)$_3$), 3.12 (s, 1H, -C*H*OSi-). ^{13}C NMR (75.4 MHz, $CDCl_3$) δ −2.45 (-Si(*C*H$_3$)$_2$(C(CH$_3$)$_3$)), 19.23 (-Si(CH$_3$)$_2$(*C*(CH$_3$)$_3$)), 26.77 (-Si(CH$_3$)$_2$(C(*C*H$_3$)$_3$)), 29.57 (-C(*C*H$_3$)$_3$), 37.70 (-*C*(CH$_3$)$_3$), 87.71 (-*C*HOSi-). HRMS (*m*/*z*): [M-1]$^+$ calcd for $C_{15}H_{33}OSi$, 257.2301; found, 257.2290. Anal. calcd for $C_{15}H_{34}OSi$: C 69.69%, H 13.26%. Found: C 69.47%, H 13.41%.

***cis*-2-*tert*-Butyl-1-(dimethylphenylsiloxy)cyclohexane (Table 4, entry 10).** ^{1}H NMR (300 MHz, $CDCl_3$) δ 0.38 (s, 3H, -SiCH_3Ph), 0.39 (s, 3H, -SiCH_3Ph), 0.86 (s, 9H, (CH_3)$_3$C-), 0.91−0.92 (m, 1H, (CH$_3$)$_3$CC*H*-), 1.13−1.31 (m, 3H), 1.45−1.76 (m, 5H), 4.22 (br s, 1H, -C*H*OSiCH$_3$Ph), 7.34−7.38 (m, 3H, Ar*H*), 7.60−7.63 (m, 2H, Ar*H*). ^{13}C NMR (75.4 MHz, $CDCl_3$) δ −1.00 (-Si*C*H$_3$Ph), −0.61 (-Si*C*H$_3$Ph), 19.97 (*C*H$_2$), 21.46 (*C*H$_2$), 26.98 (*C*H$_2$), 28.33 ((*C*H$_3$)$_3$C-), 32.50 ((CH$_3$)$_3$*C*-), 34.92 (*C*H$_2$), 51.85 ((CH$_3$)$_3$*C*CH-), 69.19 (-*C*HOSi-), 127.70 (*C*H), 129.36 (*C*H), 133.60 (*C*H), 138.95 (*C*). HRMS (*m*/*z*): [M]$^+$ calcd for $C_{18}H_{30}OSi$, 290.2066; found,

290.2063. Anal. calcd for $C_{18}H_{30}OSi$: C 74.42%, H 10.41%. Found: C 74.41%, H 10.24%.

***trans*-2-*tert*-Butyl-1-(dimethylphenylsiloxy)cyclohexane (Table 4, entry 10).** ^{1}H NMR (300 MHz, $CDCl_3$) δ 0.38 (s, 3H, -SiCH_3Ph), 0.41 (s, 3H, -SiCH_3Ph), 0.82−1.34 (m, 14H), 1.57−1.60 (m, 3H), 1.74−1.80 (m, 2H), 3.54 (td, J = 4.2, 9.9 Hz, 1H, -C*H*OSiCH$_3$Ph), 7.34−7.38 (m, 3H, Ar*H*), 7.58−7.62 (m, 2H, Ar*H*). ^{13}C NMR (75.4 MHz, $CDCl_3$) δ −1.19 (-SiCH_3Ph), −0.05 (-SiC_3Ph), 24.97 (CH_2), 26.07 (CH_2), 26.61 (CH_2), 29.17 ((CH_3)$_3$C-), 32.80 ((CH_3)$_3$C-), 37.49 (CH_2), 53.11 ((CH_3)$_3$C*C*H-), 75.13 (-*C*HOSi-), 127.73 (*C*H), 129.37 (*C*H), 133.65 (*C*H), 139.01 (*C*). HRMS (*m*/*z*): [M]$^+$ calcd for $C_{18}H_{30}OSi$, 290.2066; found, 290.2066. Anal. calcd for $C_{18}H_{30}OSi$: C 74.42%, H 10.41%. Found: C 74.35%, H 10.14%.

2-*tert*-Butyl-1-(*tert*-butyldimethylsiloxy)cyclohexane (Table 4, entry 12): *cis* isomer: ^{1}H NMR (300 MHz, $CDCl_3$) δ 0.06 (s, 6H, -Si(C(CH$_3$)$_3$)(CH_3)$_2$), 0.89 (s, 9H, -C(CH_3)$_3$), 0.90 (s, 9H, -Si(C(CH_3)$_3$)(CH$_3$)$_2$), 1.02−1.77 (m, 9H), 4.22 (br s, 1H, -C*H*OSi-). ^{13}C NMR (75.4 MHz, $CDCl_3$) δ −4.38 (-OSi-(C(CH$_3$)$_3$)(*C*H$_3$)$_2$), −3.68 (-OSi(C(CH$_3$)$_3$)(*C*H$_3$)$_2$), 18.14 (-OSi*C*-(CH$_3$)$_3$(CH$_3$)$_2$), 20.19 (CH_2), 21.54 (CH_2), 26.06 (C(CH$_3$)$_3$), 27.21 (CH_2), 28.38 (-OSi(C(*C*H$_3$)$_3$(CH$_3$)$_2$), 32.42 (-*C*(CH$_3$)$_3$), 35.27 (CH_2, *cis*), 52.30 (-*C*HC(CH$_3$)$_3$), 68.78 (-*C*HOSi-); ***trans* isomer:** ^{1}H NMR (300 MHz, $CDCl_3$) δ 0.07 (s, 6H, -Si(C(CH$_3$)$_3$)(CH_3)$_2$), 0.89 (s, 9H, -C(CH_3)$_3$), 0.95 (s, 9H, -Si(C(CH_3)$_3$)(CH$_3$)$_2$), 1.02−1.77 (m, 9H), 3.55 (td, J = 3.9, 9.4 Hz, 1H, -C*H*SiO-). ^{13}C NMR (75.4 MHz, $CDCl_3$) δ −4.03 (-OSi(C(CH$_3$)$_3$)(*C*H$_3$)$_2$), −3.51 (-OSi(C(CH$_3$)$_3$)(*C*H$_3$)$_2$), 18.06 (-OSi*C*(CH$_3$)$_3$(CH$_3$)$_2$), 24.84 (CH_2), 26.04 (CH_2), 26.06 (C(CH$_3$)$_3$), 26.57 (CH_2), 29.22 (-OSi(C(*C*H$_3$)$_3$(CH$_3$)$_2$), 32.81 (-*C*(CH$_3$)$_3$), 37.44 (CH_2), 53.17 (-*C*HC(CH$_3$)$_3$), 74.74 (-*C*HOSi-); HRMS (*m*/*z*): [M]$^+$ calcd for $C_{16}H_{34}OSi$, 270.2379; found, 270.2389. Anal. calcd for $C_{16}H_{34}OSi$: C 71.04%, H 12.67%. Found: C 71.12%, H 12.73%.

1,3,3-Trimethyl-2-(dimethylphenylsiloxy)bicyclo[2.2.1]heptane (*endo*/*exo*; 24:76) (Table 4, entry 13): *endo* isomer: ^{1}H NMR (300 MHz, $CDCl_3$) δ 0.35 (s, 6H, -Si(CH_3)$_2$Ph), 0.77 (s, 3H), 0.82 (s, 3H), 0.93 (s, 3H), 0.88−1.10 (m, 2H), 1.26−1.42 (m, 2H), 1.45−1.70 (m, 2H), 1.74−1.85 (m, 1H), 3.27 (d, J = 1.8, 1H, -C*H*OSi-), 7.35−7.39 (m, 3H, Ar*H*), 7.58−7.61 (m, 2H, Ar*H*). ^{13}C NMR (75.4 MHz, $CDCl_3$) δ −0.79 (-Si(*C*H$_3$)$_2$Ph), 19.77 (*C*H$_3$), 21.13 (*C*H$_3$), 25.35 (CH_2), 26.12 (CH_2), 30.14 (*C*H$_3$), 39.29 (*C*), 40.78 (CH_2), 48.24 (*C*H), 49.41 (*C*), 85.54 (-*C*HOSi-), 127.71 (*C*H), 129.45 (*C*H), 133.73 (*C*H), 138.60 (*C*H); one of the methyl carbon signals is overlapped with a signal for the *exo* isomer (δ −1.35 or −1.20).; ***exo* isomer:** ^{1}H NMR (300 MHz, $CDCl_3$) δ 0.35 (s, 6H, -Si(CH_3)$_2$Ph), 0.80 (s, 3H), 0.84 (s, 3H), 0.93 (s, 3H), 0.88−1.10 (m, 2H), 1.26−1.42 (m, 2H), 1.45−1.70 (m, 2H), 1.74−1.85 (m, 1H), 2.98 (d, J = 1.5 Hz, 1H, -C*H*OSi-), 7.35−7.39 (m, 3H, Ar*H*), 7.58−7.61 (m, 2H, Ar*H*). ^{13}C NMR (75.4 MHz, $CDCl_3$) δ −1.35 (-Si(*C*H$_3$)$_2$Ph), −1.20 (-Si(*C*H$_3$)$_2$Ph), 17.83 (*C*H$_3$), 24.38 (*C*H$_3$), 25.54 (CH_2), 25.76 (*C*H$_3$), 33.37 (CH_2), 41.10 (CH_2), 43.81 (*C*), 48.27 (*C*H), 49.34 (*C*), 86.80 (-*C*HOSi-), 127.71 (*C*H), 129.45 (*C*H), 133.77 (*C*H), 138.60 (*C*); HRMS (*m*/*z*): [M]$^+$ calcd for $C_{18}H_{28}OSi$, 288.1909; found, 288.1898. Anal. calcd for $C_{18}H_{28}OSi$: C 74.94%, H 9.78%. Found: C 74.99%, H 9.58%.

2-(*tert*-Butyldimethylsiloxy)-1,3,3-trimethylbicyclo[2.2.1]heptane (*endo*/*exo*; 59:41) (Table 4, entry 15). ^{1}H NMR (300 MHz, $CDCl_3$); ***endo* isomer:** δ 0.00 (s, 6H, -Si(C(CH$_3$)$_3$)(CH_3)$_2$), 0.78 (s, 3H), 0.90 (s, 9H, -Si(C(CH_3)$_3$)(CH$_3$)$_2$), 0.94 (s, 3H), 0.99 (s 3H), 0.95−1.15 (m, 2H), 1.25−1.45 (m, 2H), 1.50−1.85 (m, 3H), 3.18 (d, J = 1.5 Hz, 1H, -C*H*OSi-); ***exo* isomer:** δ 0.01 (s, 6H, -Si(C(CH$_3$)$_3$)(CH_3)$_2$), 0.86 (s, 3H), 0.90 (s, 9H, -Si(C(CH_3)$_3$)(CH$_3$)$_2$), 0.94 (s, 3H), 0.97 (s, 3H), 0.95−1.15 (m, 2H), 1.25−1.45 (m, 2H), 1.50−1.85 (m, 3H), 2.88 (d, J = 1.5 Hz, 1H, -C*H*OSi-); ^{13}C NMR (75.4 MHz, $CDCl_3$) δ −4.80 (-Si(C(CH$_3$)$_3$)(*C*H$_3$)$_2$), −4.62 (-Si(C(CH$_3$)$_3$)-(*C*H$_3$)$_2$), −4.36 (-Si(C(CH$_3$)$_3$)(*C*H$_3$)$_2$), −4.01 (-Si(C(CH$_3$)$_3$)(*C*H$_3$)$_2$), 17.91 (*C*H$_3$), 18.10 (*C*), 18.15 (*C*), 20.01 (*C*H$_3$), 21.28 (*C*H$_3$), 24.52 (*C*H$_3$), 25.28 (*C*H$_2$), 25.65 (*C*H$_2$), 25.91 (*C*H$_3$), 25.97 (*C*H$_3$), 26.00 (*C*H$_3$), 26.16 (CH$_2$), 30.41 (CH$_3$), 33.43 (CH$_2$), 39.54 (*C*), 40.81 (*C*H$_2$), 41.18 (*C*H$_2$), 44.12 (*C*), 48.30 (*C*H), 48.35 (*C*H), 49.58 (*C*), 85.07 (-*C*HOSi-), 86.24 (-*C*HOSi-); one of the quaternary carbon signals is overlapped with one of the another signals.; HRMS (*m*/*z*): [M]$^+$ calcd for $C_{16}H_{32}OSi$, 268.2222; found, 268.2223. Anal. calcd for $C_{16}H_{32}OSi$: C 71.57%, H 12.01%. Found: C 71.42%, H 11.85%.

2-[1-(Dimethylphenylsiloxy)ethyl]-1-methylpyrrole (Table 6, entry 4). ^{1}H NMR (300 MHz, $CDCl_3$) δ 0.26 (s, 3H, -Si(CH_3)$_2$Ph), 0.31 (s, 3H, -Si(CH_3)$_2$Ph), 1.52 (d, J = 6.6 Hz, 3H, -CH_3), 3.53 (s, 3H, NCH_3), 4.94 (q, J = 6.6 Hz, 1H, -C*H*OSi-), 5.98−6.02 (m, 2H, Ar*H*), 6.50 (t, J = 2.4 Hz, 1H, Ar*H*), 7.32−7.41 (m, 3H, Ar*H*), 7.50−7.56 (m, 2H, Ar*H*). ^{13}C NMR (75.4 MHz, $CDCl_3$) δ −1.54 (-Si(*C*H$_3$)$_2$Ph), −0.94 (-Si(*C*H$_3$)$_2$Ph), 23.20 (-*C*H$_3$), 33.98 (-N*C*H$_3$), 64.40 (-*C*HOSi-), 106.34 (*C*H, 2C), 122.73 (*C*H), 127.75 (*C*H), 129.49, (*C*H), 133.52 (*C*H), 138.29 (*C*), 139.20 (*C*). HRMS (*m*/*z*): [M]$^+$ calcd for $C_{15}H_{21}ONSi$, 259.1392; found, 259.1398. Anal. calcd for $C_{15}H_{21}ONSi$: C 69.45%, H 8.16%, N 5.40. Found: C 69.41%, H 8.37%, N 5.67%.

2-[1-(*tert*-Butyldimethylsiloxy)ethyl]-1-methylpyrrole (Table 6, entry 6). ^{1}H NMR (300 MHz, $CDCl_3$) δ −0.05 (s, 3H, -Si(CH_3)$_2$(C(CH$_3$)$_3$)), −0.04 (s, 3H, -Si(CH_3)$_2$(C(CH$_3$)$_3$)), 0.86 (s, 9H, -Si(CH$_3$)$_2$(C(CH_3)$_3$)), 1.51 (d, J = 6.6 Hz, 3H, -CH_3), 3.66 (s, 3H, NCH_3), 4.89 (q, J = 6.6 Hz, 1H, -C*H*OSi-), 5.96−6.02 (m, 2H, Ar*H*), 6.53 (t, J = 2.2 Hz, 1H, Ar*H*). ^{13}C NMR (75.4 MHz, $CDCl_3$) δ −5.03 (-Si(*C*H$_3$)$_2$(C(CH$_3$)$_3$)), −4.63 (-Si(*C*H$_3$)$_2$(C(CH$_3$)$_3$)), 17.93 (-Si(CH$_3$)$_2$(*C*(CH$_3$)$_3$)), 23.80 (-*C*H$_3$) 25.72 (-Si(CH$_3$)$_2$(C(*C*H$_3$)$_3$)), 34.23 (-N*C*H$_3$), 64.64 (-*C*HOSi-), 106.05 (*C*H), 106.24 (*C*H), 122.66 (*C*H), 135.76 (*C*). HRMS (*m*/*z*): [M]$^+$ calcd for $C_{13}H_{25}ONSi$, 239.1705; found, 239.1702. Anal. calcd for $C_{12}H_{22}OSSi$: C 65.21%, H 10.59%, N 5.85. Found: C 64.95%, H 10.59%, N 5.74%.

2-[1-(*tert*-Butyldimethylsiloxy)ethyl]thiophene (Table 6, entry 12). ^{1}H NMR (300 MHz, $CDCl_3$) δ 0.04 (s, 3H, -Si(CH_3)$_2$(C(CH$_3$)$_3$)), 0.08 (s, 3H, -Si(CH_3)$_2$(C(CH$_3$)$_3$)), 0.91 (s, 9H, -Si(CH$_3$)$_2$(C(CH_3)$_3$)), 1.52 (d, J = 6.3 Hz, 3H, -CH_3), 5.12 (qd, J = 0.82, 6.3 Hz, 1H, -C*H*OSi-), 6.84−6.86 (m, 1H, Ar*H*), 6.93 (dd, J = 3.4, 5.0 Hz, 1H, Ar*H*), 7.17 (dd, J = 1.2, 5.0 Hz, 1H, Ar*H*). ^{13}C NMR (75.4 MHz, $CDCl_3$) δ −5.10 (-Si(H$_3$)$_2$(C(CH$_3$)$_3$)), −4.95 (-Si(*C*H$_3$)$_2$(C(CH$_3$)$_3$)), 18.09 (-Si(CH$_3$)$_2$(*C*(CH$_3$)$_3$)), 25.68 (-Si(CH$_3$)$_2$(C(*C*H$_3$)$_3$)), 26.90 (-*C*H$_3$), 67.16 (-*C*HOSi-), 121.87 (*C*H), 123.55, (*C*H), 126.41 (*C*H), 151.76 (*C*). HRMS (*m*/*z*): [M]$^+$ calcd for $C_{12}H_{22}OSSi$, 242.11607; found, 242.11689. Anal. Calcd for $C_{12}H_{22}OSSi$: C 59.45%, H 9.15%, S 13.23. Found: C 59.18%, H 9.10%, S 13.37%.

Acknowledgment. This work was supported by the PRESTO program (JST), Grant-in-Aid for Scientific Research (B) (No. 18350047) (JSPS), and Grant-in-Aid for Scientific Research on Priority Area (No. 20037003, "Chemistry of Concerto Catalysis") (MEXT). G.H. was supported by MEXT program, Initiatives for Attractive Education in Graduate Schools (T-type Chemists with Lofty Ambition) and GCOE (Catalysis as the Basis for Innovation in Materials Science). A.O. and R.A. thank JSPS for a fellowship.

Supporting Information Available: CP/MAS NMR spectra of **1b** (^{13}C, ^{31}P and ^{29}Si) and **6b** (^{13}C and ^{29}Si). ^{31}P NMR spectra for Rh/**2** mixtures. Nitrogen adsorption−desorption isotherms and pore diameter distributions for silica gel 60N, CARiACT Q-10, **1a** and **1b**. This material is available free of charge via the Internet at http://pubs.acs.org.

OM800683G